J. Anat. (1998) **193**, pp. 251–272, with 12 figures Printed in the United Kingdom

Facial growth in *Cercocebus torquatus*: an application of three-dimensional geometric morphometric techniques to the study of morphological variation

PAUL O'HIGGINS AND NICHOLAS JONES

Evolutionary Anatomy Unit, Department of Anatomy and Developmental Biology, University College, London, UK

(*Accepted 19 May 1998*)

ABSTRACT

This paper presents a study of 3-dimensional growth in the facial skeleton of the mangabey, *Cercocebus torquatus*. The pattern of facial cortical remodelling in this species is already well mapped from an earlier study. In this paper we consider the extent to which these remodelling maps relate to ontogenetic changes in size and shape of the face. This study is based on 31 facial landmarks taken from 49 adult and subadult faces. Our analysis draws on some of the tools of geometric morphometrics and we take this opportunity to describe our implementation of these tools for 3D data. The geometric analysis permits the known remodelling maps to be interpreted in the context of the general pattern of facial growth in this species. We are also able to examine sexual dimorphism in the face of this species and consider the extent to which males and females share similar ontogenetic allometries. Our findings indicate that the general pattern of size-related shape variation during facial growth is more or less identical for males and females up to eruption of the third permanent maxillary molar (M3). After this, ontogenetic allometries appear to diverge. The finding of a common growth allometry that is well approximated for younger specimens by a simple linear model is consistent with the earlier findings of a consistent pattern of facial remodelling up to M3 eruption. We consider the implications of these findings in terms of the potential for these approaches in the study of comparative growth in related species.

Key words: Facial remodelling; geometric morphometrics; thin plate spline analysis.

INTRODUCTION

Evolutionary transformations in craniofacial form come about through ontogenetic modifications. As such, the phylogenetic interpretation of morphological differences between adults must draw on knowledge of comparative ontogeny. This, in turn, depends on adequate quantitative morphological analysis. In this paper we outline our implementation of some of the methods of geometric morphometrics and illustrate its application in the study of 3-dimensional (3D) growth patterns in the primate face. The primate we examine is the mangabey, *Cercocebus torquatus*, because the pattern of facial cortical remodelling during growth in this species is well-established (O'Higgins et al. 1991). The aim of this study is to examine growth variation in facial morphology in this species. The biological issues we address are (1) the relationship between remodelling patterns and patterns of morphological change in the face during growth and (2) the ontogenetic basis of sexual dimorphism in the face of this species.

The ontogenetic basis of craniofacial variation

Craniofacial growth proceeds through the co-ordinated displacement of skeletal elements and remodelling of bone surfaces (Enlow, 1966). These processes are influenced in different regions according to the genetic program determining the form of especially the primary cartilaginous elements of the skull, soft tissue growth, dental development, functional and soft tissue spaces, and hormonal and biomechanical influences. The skull can therefore be

Correspondence to Dr P. O'Higgins, Department of Anatomy and Developmental Biology, University College London, Rockefeller Building, University Street, London WC1E 6JJ, UK.

modelled as a number of functional matrices (Moss & Young, 1960), each subject to a mix of influences which determine the local pattern of displacements and remodelling and which to some degree influence the growth of other units.

Differences in the directions, rates and relative timing of growth at different sutures together with differences in timings, locations, shapes, sizes, types and rates of remodelling activity in different regions combine to underpin morphological differences between adult crania (Enlow, 1966; Krogman, 1974). Therefore, in considering the significance of morphological differences between adults an understanding of the ontogenetic basis of these differences in terms of patterns of growth is likely to be important.

Craniofacial skeletal growth is directed and influenced by soft tissue growth, dental maturation and the biomechanical and hormonal milieu (Enlow, 1968, 1975). Remodelling of the bone surface contributes, together with sutural growth, to the normal development of the sizes and shapes of the bones of the face and vault. This ontogenetic remodelling process is termed 'bone growth remodelling' (Bromage, 1986). It is a process which is said to act to a large extent as a compensatory mechanism maintaining proper bone alignment, function and proportionate growth during bone displacement (Enlow, 1975). The surface distribution of bone growth remodelling processes is therefore considered to be an important indicator of craniofacial growth as a whole (Enlow, 1975; Bromage, 1986). It is currently hypothesised that growth remodelling acts as a compensatory mechanism to maintain proper bone alignment during displacement (Enlow, 1968, 1975). Consequently it has been suggested that the spatial distribution, direction and rate of surface remodelling activity should serve as an indication of the pattern of displacement (Enlow, 1975; Bromage, 1986).

It is a fairly simple, although time consuming matter to map out bone growth remodelling activity in the face since it is essentially a surface phenomenon. Rather than take many sections of a face and examine these under the light microscope, surfaces can be examined nondestructively using the scanning electron microscope (SEM). Boyde & Jones (1972) have demonstrated the characteristic surface features of forming, resting and resorptive bone surfaces as observed under the SEM and Bromage (1986) has developed a technique to allow remodelling activity to be mapped on high resolution replicas under the SEM.

To date the patterns of bone growth remodelling (deposition and resorption) are only known for a few primates (humans: Enlow, 1975; rhesus macaque: Enlow, 1966; chimpanzee: Johnson et al. 1976; *Australopithecus*: Bromage, 1986; sooty mangabey, *Cercocebus torquatus atys*: O'Higgins et al. 1991). It is known from these studies that there are some inter- and intraspecific differences in craniofacial remodelling. The question arises as to the extent to which these indicate differences in patterns of overall growth.

What might we learn by studying facial growth in Cercocebus torquatus*?*

In the sooty mangabey, O'Higgins et al. (1991) have demonstrated that remodelling fields are relatively constant in their location, size and type of activity (depository or resorptive) between individuals of different ages (ranging from completion of deciduous dentition to appearance of the third permanent maxillary molar – M3; Fig. 1). From this finding it can be hypothesised that the patterns of bone displacement during this period of ontogeny are also relatively constant.

No test of the hypothesised relationship between bone displacements and remodelling activity in the face has ever been undertaken. This is because it is impossible to produce satisfactory 3D models of morphological change due to bone displacements alone. O'Higgins & Dryden (1992) have used relatively new techniques of statistical shape analysis applied to the study of anatomical landmarks to examine some aspects of craniofacial growth in the sooty mangabey using 2-dimensional data. In this paper we present an extension of this work into 3 dimensions which draws upon more recent advances in the analysis of shape variation to generate a statistical model of 3D allometry in the face of this species.

Since this model depends on landmarks that are sited on bone surfaces (either resting or undergoing remodelling) and sutural junctions, it will reflect landmark movements due to both remodelling and sutural growth. Given that remodelling activity in this species remains more or less constant during the period of growth, spanning completion of deciduous dentition to appearance of M3, we expect a uniform ontogenetic allometry during the same period. By this we mean that we expect the overall pattern of growth (due to displacement and remodelling) to generate shape changes which are consistent throughout this growth period. Such a consistent pattern would be fully described by a linear model of shape variation with increasing size (allometry).

Thus we are able to test the hypothesis that

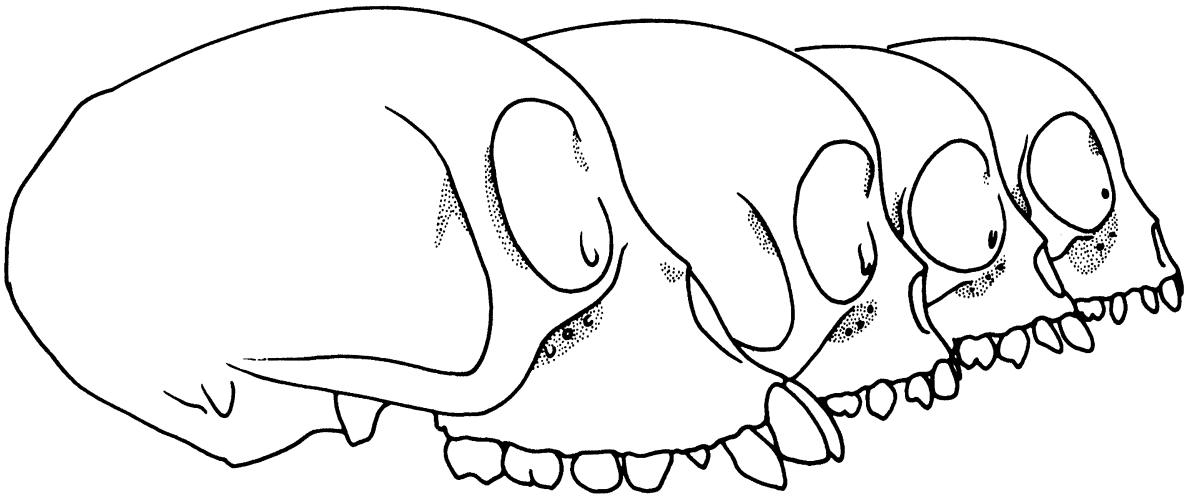

Fig. 1. Remodelling maps from an age series of *Cercocebus torquatus*. Stipple, resorptive; white, depository. Rightmost specimen, youngest; deciduous dentition erupted and all but dm1 in occlusion. Middle specimens, intermediate, full deciduous dentition. Leftmost, oldest, possessing full permanent dentition except canines and third molar.

consistency of remodelling activity indicates consistency of ontogenetic allometries. This hypothesis would be falsified by the finding that shape variation with increasing size between completion of deciduous dentition and M3 appearance cannot be explained by a linear model.

Statistical growth models allow us to test a further hypothesis: that the ontogenetic (growth) allometries of males and females are identical such that differences between the sexes arise simply through truncation of this allometry in females relative to males (or extension in males relative to females). This question has never been investigated in this species although the ontogeny and nature of craniofacial sexual dimorphism in monkeys and apes has been addressed by several workers (e.g. Schultz, 1962; Wood, 1975, 1976, 1985; in hominoids: Shea, 1983, 1986; O'Higgins et al. 1990; Wood et al. 1991; in monkeys: Cheverud & Richtsmeier, 1986; Leigh & Cheverud, 1991; Corner & Richtsmeier, 1991, 1992, 1993; Richtsmeier et al. 1993*a*). In general it appears that cranial sexual dimorphism, where it exists, in monkeys and apes arises through ontogenetic scaling such that male and female adult morphologies represent different endpoints on a single ontogenetic allometry with female adults usually being smaller than males. Sexual differences in endpoint might, in turn, arise through sexual differences in the rate of growth; rate hypermorphosis, or in the duration of growth; time hypermorphosis, or through some combination of rate and time differences between the sexes (Shea, 1983, 1986).

This study therefore sets out to test 2 hypotheses: first that the general growth pattern of the face of *Cercocebus torquatus* is more or less constant from completion of the deciduous dentition to eruption of M3 as seems to be indicated by the stability of remodelling activity throughout growth. Second that in this species, sexual differences in adult facial morphology arise entirely through ontogenetic scaling. The first hypothesis will be falsified if we are able to demonstrate variations in growth allometry (shape changes with increasing size during the relevant period of growth); the second if we are able to demonstrate differences between the growth allometries of males and females.

MATERIALS

The sample of *Cercocebus torquatus* used in this study comprises 49 individuals in total, 37 (*Cercocebus torquatus* atys) curated in the Department of Anatomy and Developmental Biology, University College London and 12 (*Cercocebus torquatus torquatus*) in the Natural History Museum, London. Of this sample, 17 are known to be male from field records; 24, female and 8 are of unknown sex. 7 of the males and 8 of the females are adults whilst the remaining specimens range between infancy and adulthood. Subspecies were pooled after preliminary analyses demonstrated that their faces are indistinguishable on the basis of the landmarks used in this study. Details of these specimens and, to allow the reader to judge the age range, of their maxillary dentition are given in Table 1.

Table 1. *Sample of Cercocebus torquatus used in this study: rank order age based on dental eruption:*

Catalogue number and location All UCL = *torquatus atys* except $^{+}$ = NHM = *torquatus torquatus*	Maxillary dentition	Sex
$^{+}$ZD1954.925	Di1,Di2,Dc,Dm1	M
$^{+}$ZD1954.929	DM2 erupting	M
C13.5	DM2 almost in full occlusion	?
$^{+}$ZD1954.927	DM2 almost in full occlusion	M
$^{+}$ZD1954.926	Full deciduous	M
$^{+}$ZD1954.928	Full deciduous	M
C 13.6	Full deciduous	?
C 13.7	Full deciduous	?
C 13.41	M1 deep in crypt	?
C 13.39	M1 deep in crypt	M
$^{+}$ZD1954.932	M1 in crypt	F
C 13.43	M1	?
C 13.36	M1	F
C 13.45	M2 v deep crypt; I1 erupting	F
C 13.40	M2 deep in crypt; I1 erupted	?
$^{+}$ZD1971.2317	M2 deep in crypt; I1 erupted; I2 erupting	M
C 13.8	M2 deep in crypt; I1 erupted; I2 erupting	F
C 13.42	M2 deep in crypt; I1 erupted; I2 erupted	F
C 13.33	M2 in crypt; I1 erupted; I2 erupted	F
C 13.34	M2 erupting; I1 and I2 erupted	F
C 13.9	M2 erupting; I1 and I2 erupted	?
C 13.17	Adult pM1, pM2, M1, M2, I1, I2 erupted and in occlusion	?
C 13.1	Adult pM1, pM2, M1, M2, I1, I2 erupted and in occlusion	F
C 13.31	Adult pM1, pM2, M1, M2, I1, I2 erupted and in occlusion	F
C 13.32	Canine erupting	F
C 13.35	Canine almost fully erupted	F
C 13.14	Canine fully erupted, M3 in crypt	F
C 13.11	Canine fully erupted, M3 in crypt	F
C 13.15	Canine fully erupted	F
$^{+}$ZD1954.930	M3 in crypt	F
C 13.27	M3 erupting	F
C 13.3	M3 erupting	F
C 13.20	M3 erupting	M
C 13.26	M3 almost in occlusion	M
$^{+}$ZD1954.931	Full adult	F
C 13.12	Full adult	F
C 13.29	Full adult	F
C 13.30	Full adult	F
C 13.2	Full adult	F
C 13.4	Full adult	F
C13.28	Full adult	F
$^{+}$ZD1855.12.26.28	Full adult	F
$^{+}$ZD1932.6.19.1	Full adult	M
$^{+}$ZD1944.69	Full adult	M
C 13.21	Full adult	M
C 13.22	Full adult	M
C 13.23	Full adult	M
C 13.24	Full adult	M
C 13.18	Full adult	M

METHODS

Overview of methodology

The shape of each face is described by the 3D coordinates of 31 facial landmarks that can be reasonably considered developmentally homologous. The landmark configurations are used to calculate a measure of overall scale, centroid size and then are scaled, translated and rotated such that they 'best fit' each other. These fitted configurations are used to estimate a mean configuration (mean shape) and, after suitable statistical manipulation (see below) the

principal components (PCs) of shape variation are calculated. Scores of specimens on these PCs are then examined for evidence of size or sex related variation. Where such evidence is found its nature is explored by visualising 3D reconstructions of faces representing variation along PCs. Further visualisations of growth allometry and sexual dimorphism are undertaken using cartesian transformation grids.

Since the methods employed are relatively new they are discussed below at some length. Formulae are kept to a minimum and pictorial and verbal descriptions are provided in order to inform the nonmathematician whilst full references are provided to the detailed statistical literature relevant to this approach to shape analysis.

Details of methodology

Measurement and precision of measurement

The aim of this study is to examine growth variation in facial morphology in this species. The quantitative analysis of morphological variation is an important issue which has been addressed in many contexts (Sneath & Sokal, 1973; Sneath, 1967; Bookstein, 1989; Lele, 1993; Marcus et al. 1996; Dryden & Mardia, 1998). Numerous approaches are in common use (reviewed in O'Higgins, 1997). These can be divided into those that describe outline or surface morphology on the basis of landmarks and those with less dependency on landmarks.

Landmark based analyses inevitably omit information about the regions between landmarks but they allow interpretations of morphological differences to be made with respect to equivalent points and, by inference, the regions delimited by these points. Where form is studied without reference to landmarks interpretation of morphological variations can only be in terms of general as opposed to local features of form, elongation, undulation, etc. Any attempt to interpret variations quantitatively in terms of differences in equivalent local regions is prohibited by the failure to define such equivalences (e.g. as landmark locations) in the first place. This concept is well illustrated by the technique of Fourier analysis. Fourier coefficients can be used to estimate overall differences in shape but any attempt at interpretation of the localisation of these differences is foiled by the nature of the coefficients themselves; they relate to the frequency, not the spatial, domain. This argument is presented more fully in O'Higgins (1997). It leads us to describe facial morphology in our sample in terms of the x, y and z coordinates of equivalent points on the face of each individual.

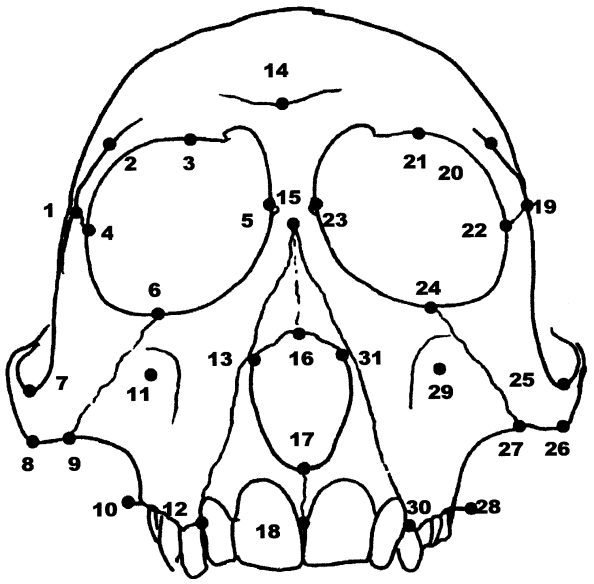

Fig. 2. Landmarks used in this study. See Table 2 for definitions.

The notion of equivalence is problematic. At its most basic level each landmark indicates our best estimate of the location of bony material which has arisen in each individual through equivalent morphogenetic processes. As such we have selected landmarks that can reasonably be considered developmentally homologous. They are based on knowledge of comparative anatomy and developmental biology. The landmarks we select are so designed that they allow a reconstruction of facial morphology through a wire frame model and rendered surfaces. Some landmarks are of type I (Marcus et al. 1996) some of type II and others are of mixed type I/II. Type I landmarks are those whose equivalence from specimen to specimen is supported by the strongest local evidence, for instance the meeting of structures, whilst type II landmarks are those whose equivalence is supported by geometric rather than compositional evidence, such as the tips of bony prominences. The 31 landmarks used in this study are shown in Figure 2 and are defined anatomically in Table 2.

The 3D coordinates of these landmarks were taken using a Polhemus 3 Space Isotrak II digitiser (Polhemus Incorporated, 1 Hercules Drive, PO Box 560, Colchester, VT 05446, USA) which operates electromagnetically through detection of the location and orientation of a coil within a pointing stylus relative to 3 reference coils. Tests of accuracy using a cube of known dimensions indicate that measurements of coordinates are accurate to within approximately 0.5 mm although this figure varies according to ambient electromagnetic conditions.

Precision of measurement was assessed by measuring 2 similar specimens 5 more times (6 sets of

Table 2. *Definitions of landmarks*

Number	Definition: based on anatomical orientation of the face
1 & 19	Most lateral point on zygomaticofrontal suture on orbital rim
2 & 20	Most superolateral point on supraorbital rim
3 & 21	Uppermost point on orbital aperture
4 & 22	Zygomaticofrontal suture at the lateral aspect of the orbital aperture
5 & 23	Frontolacrimal suture at medial orbital margin
6 & 24	Zygomaticomaxillary suture at inferior orbital margin
7 & 25	Superior root of zygomatic arch
8 & 26	Inferior root of zygomatic arch
9 & 27	Zygomaticomaxillary suture at root of zygomatic arch
10 & 28	Most posterior point on maxillary alveolus
11 & 29	Deepest point in maxillary fossa
12 & 30	Maxillary-premaxillary suture at alveolar margin
13 & 31	Nearest point to maxillary-premaxillary suture on nasal aperture
14	Upper margin of supraorbital rim in the midline
15	Nasofrontal suture in the midline
16	Tip of nasal bones in the midline
17	Premaxillary suture at the inferior margin of the nasal aperture in the midline
18	Premaxillary suture at alveolar margin

measurement being taken on these specimens in all). These repeats were submitted to geometric morphometric analyses as described below in order to assess variation due to errors of precision in relation to variability of the sample as whole.

Morphometric analysis

In our analysis of morphological variation we seek methods which preserve geometric information throughout the analysis. We turn to the class of approaches increasingly referred to as geometric morphometrics or statistical shape analysis (Rohlf & Bookstein, 1990; Marcus et al. 1996; Dryden & Mardia, 1998). These methods have been developed statistically over the last 10–15 y (see Dryden & Mardia, 1998). They draw their motivation from the classic suggestions for the study of deformations of Thompson (1917) in which form differences are represented as deformations of a cartesian grid. In this paper we give an overview of the methods we employ, our aim being to introduce them to the general reader. They are highly mathematical and for reasons of brevity we include only the most pertinent formulae.

The task of describing relative landmark movements has proven intractable until recently. The main difficulty has been that any attempt to analyse differences between forms by superimposing one upon the other suffers from the problem of registration (here form is defined as the morphology of an object, including its scale but not its location or orientation; the term shape is used to refer to aspects of form independent of scale). All landmarks will appear to 'move away' from the reference points chosen for the superimposition. Different registrations will appear to indicate different patterns of growth. One significant early attempt to deal with these issues is that of Sneath (1967) who used a least squares superimposition method to obtain sensible registrations before constructing cartesian transformation grids using cubic splines. Wider acceptance of his general scheme of analysis was hampered by lack of a thorough statistical and geometric underpinning and by available computational power.

In an extensive series of studies Richtsmeier and coworkers have examined the geometry of craniofacial growth in several species of Old and New World monkey. The methods used in these studies include finite element scaling (FESA: Cheverud et al. 1983; Cheverud & Richtsmeier, 1986; Richtsmeier, 1989) which is used to generate representations of landmark displacements as deformations. FESA, however, suffers from the difficulty that several relatively simple elements are used to subdivide the objects under study. Consequently, patterns of shape difference may appear to show discontinuities at element boundaries.

In more recent studies by Richtsmeier and her coworkers the subject of statistical analysis is inter-landmark distances (ilds) rather than cartesian coordinates. The methods they use are collectively known as Euclidean Distance Matrix Analysis (EDMA; Lele, 1993). These examine differences between specimens in terms of ratios between equivalent ilds. EDMA is usually applied to sets of ilds representing every possible distance between the chosen landmarks since such a set enables complete reconstruction of landmark coordinates. The result is that very large matrices of ild ratios have to be interpreted. An alternative would be to subdivide the landmark set into tetrahedra designed so that landmark coordinates can be reconstructed on the basis of a much smaller set of ilds. This would simplify analysis but different tetrahedral configurations might influence the analytical outcome.

In examining ilds rather than coordinates in studies of shape variation issues concerning registration are avoided, however, visualisation and interpretation of results is somewhat more difficult and issues relating to the estimation of means, selection of ilds and choice of scaling method arise. Lele (1993) argues strongly in favour of EDMA and against registration based approaches such as those used in this study. Many other statisticians and biometricians place confidence

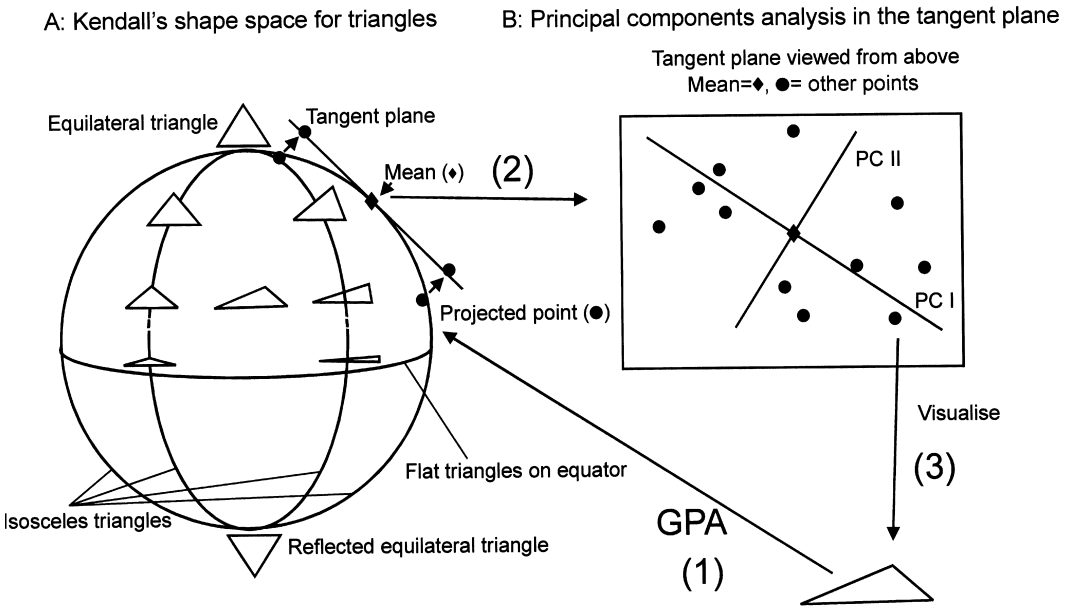

Fig. 3. (*A*) Approximate sketch of Kendall's shape space for triangles. Equilateral triangles lie at the poles, the southern hemisphere is a reflection of the northern. The sphere is divided into 12 equal half lunes (6 in each hemisphere); if the apices of the triangles are unlabelled and reflections are ignored all triangles lie in one half lune. Isosceles triangles lie along the lines dividing lunes and flat triangles at the equator. (*B*) Schematic indicating the projection of points representing triangles in Kendall's shape space into a space tangent to the mean triangle (arrows) and the principal components of shape variability (PC I, PC II) in this tangent space. The steps involved in the analyses used in this study are numbered. (1) Generalised Procrustes analysis (GPA) is used to register figures; these are then represented as points in the shape space. (2) Points are projected into a space tangent to the mean and the principal components (PCs) of shape variation in this space are extracted. (3) Visualisation of the shape variability represented by PCs is achieved by reconstruction of figures.

in registration based approaches (see for example Bookstein, 1978, 1987; Marcus et al. 1996; Dryden & Mardia, 1998). Only one thing is certain; there is no absolute agreement as to which approach is best suited to which circumstances.

Size

In analyses of form (size plus shape) based on landmark coordinates such as are undertaken here, a mathematically natural size measure is centroid size (Dryden & Mardia, 1998), S(X), which is the square root of the sum of squared euclidean distances from each landmark to the centroid (mean of landmark coordinates).

$$S(X) = \sum_{i=1}^{k}\sum_{j=1}^{m}(X_{ij}-\bar{X}_j)^2.$$

X is a $k \times m$ matrix of the cartesian coordinates of k landmarks in m real dimensions it has i, jth elements X_{ij} and $\bar{X}$ is an $m \times 1$ matrix of mean coordinates representing the centroid it has jth element $\bar{X}_j$.

Registration and shape spaces

Generalised Procrustes analysis registers series of forms by removing translational and rotational differences and scaling them such that they best fit (Gower, 1975; Rohlf & Slice, 1990; Goodall, 1991). GPA registers n specimens, each represented by a $k \times m$ matrix of landmark coordinates, X_i, $i = 1, \ldots, n$. The registered specimens are denoted, X'_i, and the sum of squared differences, d^2, between them is minimised.

$$d^2 = \sum_{i=1}^{n}\sum_{j=i+1}^{n}(X'_i - X'_j)^2.$$

The registered landmark configurations can be represented as points in a shape space which is of lower dimensionality than the figure space ($= km$ dimensions) since location (m dimensions), rotation ($m(m-1)/2$ dimensions) and scale (1 dimension) differences have been removed. For 2-dimensional data the space is therefore of dimensionality km-4 and for 3 dimensional, km-7.

This space was first described by Kendall (1984) and it is commonly referred to as Kendall's shape space. The relative locations of points representing specimens in this space are more or less independent of registration if variations are small. Additionally and importantly from a statistical perspective isotropic distributions of landmarks about the mean result in an isotropic distribution of points representing specimens in the shape space. Kendall's shape space is however noneuclidean (nonlinear). For populations of triangles the space can be visualised as being spherical (Fig. 3*a*) but for more than 3

landmarks the space is much more complex being high dimensional (Le & Kendall, 1993).

Since the shape space is nonlinear, great care is needed in carrying out statistical analyses. One approach which is particularly appealing since it naturally allows the study of multivariate allometry, is to carry out principal components analysis (PCA) in the tangent plane to Kendall's shape space (Dryden & Mardia, 1993; Kent, 1994). For triangles we take the scatter of points on the spherical shape space representing variation within our sample and project it into a euclidean tangent plane in exactly the same way as a cartographer might project a map from a globe onto a flat sheet of paper (Fig. 3*b*). The coordinates of the points representing specimens are no longer given in terms of the sphere, but rather as coordinates in the plane. As long as the projection has not resulted in excess distortion (as might occur if the projection encompasses a large proportion of the sphere) we can carry out useful analyses in this plane. For higher dimensions the tangent plane to the shape sphere can be imagined as a tangent space of $km-m-m(m-1)/2-1$ dimensions.

Procrustes tangent coordinates can be estimated simply as the km vector of deviations from the mean of the Procrustes registered coordinates. Alternatively the partial Procrustes tangent space projection given by Dryden & Mardia (1993) may be used. This projection results in a $(k-1)m$ vector of tangent space shape coordinates with respect to the mean for each specimen. Both of these vectors of tangent space coordinates are rank $km-m-m(m-1)/2-1$. Principal components analysis can be carried out using tangent space coordinates to extract $km-m-m(m-1)/2-1$ eigenvectors, which are the principal components of variation of shape (Fig. 3*b*). For a growth study we expect that the first few principal components will serve as an adequate model of allometry. Note that, since Procrustes analysis involves scaling, the variations we examine through PCA are shape rather than form variations. If we wish to examine the relationship between size and shape (allometry) we can do this by examining plots and correlations of principal component (PC) scores vs centroid size for the significant principal components.

The question arises as to how we might assess if variations are small (i.e. if data are concentrated) enough to enable us to confidently interpret the results of our analyses as being more or less independent of registrations. In this study we carry out generalised Procrustes analysis (GPA) of all 49 specimens to generate km registered x, y and z coordinates per specimen. We then carry out 2 PCAs; one of residuals of these coordinates from the Procrustes mean (simple tangent space projection) and the other (which we refer to as PCAt) of the vector of $(k-1)m$ tangent space coordinates calculated using the tangent space projection given by Dryden & Mardia (1993). The discrepancies between these PCAs, particularly in the disposition of specimens furthest from the mean, to some degree give an indication of the concentration of the data; just as distinct cartographic projections will produce different maps if the projected region covers a large part of the globe. If both analyses produce similar results it is likely our data are concentrated in the shape space.

In addition we carry out GPA and PCAt of the whole sample plus 5 repeat sets of measurements taken on 2 specimens as a test of technique. This analysis allows us to assess the magnitude of errors of precision relative to the differences in shape between these 2 specimens and within the sample.

Visualisation

Since the PCs are mutually orthogonal they each represent statistically independent modes of variation in the sample. Further interpretation of the PCs depends on visualisation of the shape variation represented by each. Shape variability explained by each PC can be readily visualised by reconstructing hypothetical forms x_h along it. The mean coordinates (e.g. x_{mean}, a vector, length km) are added to the product of the PC score of the hypothetical specimen (c) and the eigenvectors (γ) for the PC of interest.

$$x_h = x_{\text{mean}} + c\gamma.$$

If the PCA is based on tangent space coordinates a projection of those of the hypothetical specimen into configuration space (the space of the original specimens) is also carried out. Such reconstructions of transformed means allow variability to be represented pictorially and series of such transformed means can be combined to produce an informative 'morphing' animation of shape variation.

These visualisations can be further interpreted using cartesian transformation grids calculated from triplets of thin-plate splines (TPS; Bookstein, 1989; Marcus et al. 1996; Dryden & Mardia, 1998). The resulting grids do not suffer from the problems of element design and discontinuity between elements encountered in FESA; instead, the grids are derived from a smooth mathematical function applied to the whole landmark configuration. The grids derived from TPS indicate how the space surrounding a reference shape might be deformed into that sur-

rounding a target shape such that landmarks in the reference map exactly into those of the target. The thin plate spline ensures that this deformation involves minimum bending. It is chosen for this purpose since the grid fits the landmarks exactly and is bent minimally between. The statistical and graphical models of shape transformations which result from these approaches are readily interpretable and highly visual (e.g. Bookstein, 1978, 1989; Marcus et al. 1986; O'Higgins & Dryden, 1992, 1993).

Implementation of morphometric methods

The analyses described in this paper were carried out using a personal computer and software specially written for this purpose by the authors.

The suite allows raw 2 or 3D cartesian coordinates to be registered through generalised Procrustes analysis. Following GPA, tangent space projections may be undertaken and a principal components analysis carried out. Output appears in several linked windows which enable interactive exploration of shape variability. The basic descriptions of specimens together with any independent variables such as centroid size, age, etc. are displayed in a window. Another window offers plots of pairs of PCs or of any one PC vs centroid size or other independent variable. Numerical results of GPA and PCA are presented in another window. A further window is a 3-dimensional viewer which allows the user to visualise landmark configurations, wireframe models based on these configurations or surface rendered visualisations of landmark configurations. A control window allows the user to investigate the variability displayed in the PC plots by interactively 'sliding' the mean configuration up and down any chosen PC. The result is that the mean configuration shown in the viewer 'warps' or 'morphs' according to the position it represents on the PC under examination. This facility is extended such that, using a mouse, the shape represented by any chosen point in the PC representation of shape space can also be viewed. By moving the mouse control around the PC plot the relationship between shapes and the projected shape space can be readily understood. One further control allows 2 or 3 dimensional cartesian transformation grids to be calculated between reference and target forms using thin plate splines. The reference form is selected first by pointing the mouse at any point of interest in the PC plot and square or cubic grid is drawn in its vicinity. The target form is also chosen by pointing the mouse and a deformed transformation grid is drawn in its vicinity. The grid can be scaled and otherwise manipulated to facilitate understanding of the shape differences between target and reference.

All the numerical computations underpinning our suite have been thoroughly tested by comparing the results obtained from test data with those obtained using other available packages. Where no comparable package was available we have consulted widely with colleagues (see Acknowledgements) and both authors have thoroughly proofed each other's work.

RESULTS

Precision of measurement

The 5 repeat sets of coordinate data from the 2 test specimens together with the data from the 49 study specimens were submitted to GPA and PCAt. The first 2 principal components from this analysis are plotted in Figure 4. PC I accounts for 55% and PC II for 8% of the total variance in the sample. In this plot the 6 instances of each of the test specimens (5 repeats plus original) are plotted in black. The other specimens (1 set of measurements from each) are plotted as open circles. The black markers are tightly clustered with several test repeats plotting directly on top of each other. This indicates that errors of precision are small with respect to sample variability and are unlikely to have unduly influenced our results.

Concentration of data and tangent space projections

One issue that concerns us is the extent to which our chosen superimposition of coordinates and analytical method might lead to unreasonable conclusions. Dryden & Mardia (1998) and Lele (1993) have discussed this issue in detail. In essence, our analysis of coordinates after registration depends on the variation within the sample being small relative to the variation amongst all possible 3D shapes with 31 landmarks. If variability is, indeed, relatively small, the specimens are concentrated in Kendall's shape space and PCA in the tangent space is feasible. If the data are relatively concentrated we can also be confident that the chosen registration method is not unduly influencing results since any reasonable registration can be expected to result in an approximately similar scatter of specimens. Common sense indicates that the shapes of the faces of sooty mangabeys as defined by 31 3D coordinates must represent a very small fraction of all possible shapes defined in 31 coordinates in 3D. A quantitative assessment of concentration is, however, also desirable.

The extent to which the result from PCA of data derived from GPA differs from that of PCAt (Dryden

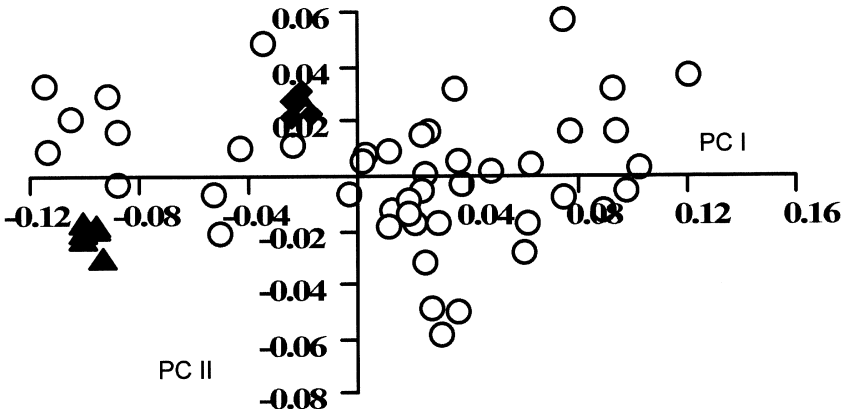

Fig. 4. Test of technique. The 5 repeats of each of specimens 3.7 and 3.36 together with the data from the 49 specimens selected for the full analysis are submitted to PCAt. PC I is plotted on the horizontal axis and PC II on the vertical. The 6 separate instances of measurements from specimens 3.7 and 3.36 (5 repeats plus 1 original set of landmark coordinates) are represented by black triangles and black diamonds respectively. The remaining specimens are represented by open circles. The repeats cluster tightly relative to the variation present in the sample as whole.

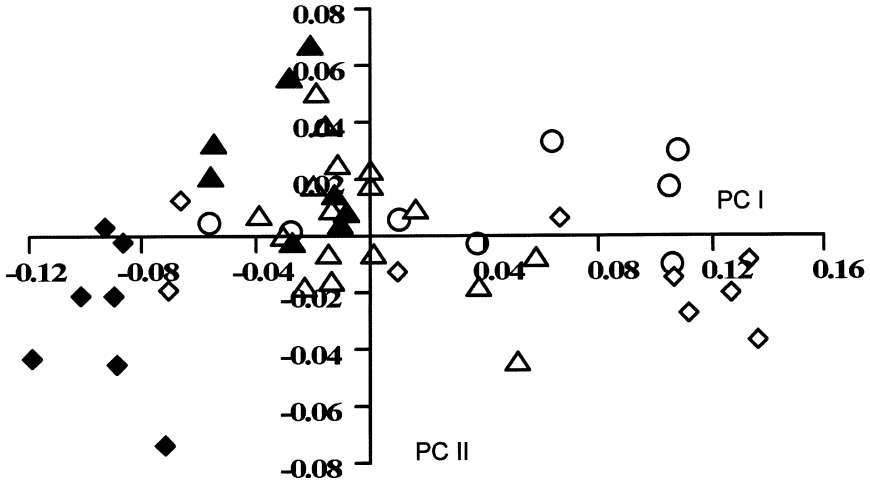

Fig. 5. Principal components analysis of 93 Procrustes registered coordinates. PC I (horizontal axis) vs PC II (vertical axis) for the whole sample. Diamonds, males; triangles, females; circles, sex unknown; black markers, adults.

& Mardia's (1993) partial Procrustes tangent projection) serves to indicate concentration in that differences in result between these 2 approaches arise because of differences in the method of projection into the tangent space. The less concentrated the data the greater the difference we expect from different projections especially in the relations of those specimens furthest from the mean. The results of PCA and of PCAt are presented as plots of PC I vs PC II in Figures 5 and 6. At first glance they appear different but careful examination shows that this difference is simply a matter of reflection of PC scores. In fact in every detail the 2 analyses are more or less identical. Numerically the eigenvalues for the PCs in the 2 analyses differ only in the 4th decimal place or higher and the PC scores are likewise nearly identical in all but sign. This finding leads us to conclude that the data are highly concentrated; differences in the ways we project into a tangent space make hardly any difference to our results, indeed they lead us to identical biological conclusions.

We do not test the effects of different 'reasonable' registrations explicitly here since the properties of the resulting shape spaces are extremely complicated and, given concentrated data, we do not expect they would lead to any difference in our biological conclusions. We intend, however, to explore this issue explicitly in a future paper. For now we make the point that as biologists we are concerned that the methods we use are reasonable and that the errors we might introduce by choosing one set of approaches over another are small with respect to the phenomena we study. For the purposes of this study we are satisfied on both counts. In other studies, findings with respect to concentration may be more worrying. In such cases we propose that several approaches be used sim-

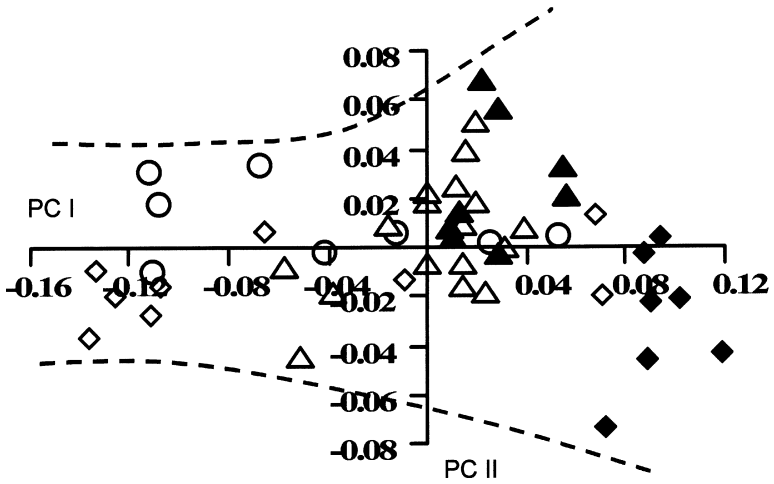

Fig. 6. Principal components analysis of 90 tangent space coordinates (PCAt). PC I (horizontal axis) vs PC II (vertical axis) for the whole sample. Diamonds, males; triangles, females; circles, sex unknown; black markers, adults. Dashed lines indicate limits of distribution of sample on PC II.

Table 3. *Eigenvalues of first 10 PCs from the analysis of tangent space projected coordinates*

Principal component	Eigenvalue	Proportion of total variance	Cumulative proportion
PC 1	0.004541371	0.52	0.52
PC 2	0.000716891	0.08	0.60
PC 3	0.000430912	0.05	0.65
PC 4	0.000327163	0.04	0.69
PC 5	0.000300155	0.03	0.72
PC 6	0.000273133	0.03	0.75
PC 7	0.000219557	0.02	0.77
PC 8	0.000208227	0.02	0.80
PC 9	0.000171020	0.02	0.82
PC 10	0.000149637	0.02	0.84

ultaneously and that only those findings common to each method be reported with confidence.

It matters not at all which method of tangent space projection we use in this study since the data are concentrated but, for the purposes of statistical nicety we present below only results from PCAt (after the recommendations of Mardia & Dryden, 1993; Dryden & Mardia, 1998).

Patterns of variation within our sample

The plot of PC I vs PC II shown in Figure 6 gives the clear impression that PC I accounts for a much larger proportion of the sample variance than does PC II. This is confirmed by reference to the eigenvalues given in Table 3 which shows that PC I accounts for 52%, PC II for 8% and subsequent PCs for a diminishing proportion of overall variance; 90% of the sample variance is explained by 15 PCs and 99% by 36.

Specimens appear to be ordered along PC I according to sex and also age (Fig. 6). Thus younger individuals are towards the left (increasingly negative scores on PC I) as are adult females with respect to adult males. The relationship between the size and shape of crania was investigated by looking for evidence of a significant correlation between the scores of individuals on each PC and centroid size. Through this procedure we effectively examine the principal vectors of variation in shape space for evidence of allometry. Only on PC I was there any evidence of such an allometric trend. Scores on PC I vs centroid size are plotted in Figure 7. This plot indicates that a convincing linear relationship exists such that small individuals have low scores on PC I and vice versa. The correlation between centroid size and scores on PC I is 0.95 and this relationship is highly significant ($P < 0.001$). Furthermore PC I accounts for 52% of total shape variance in the sample so we conclude that ontogenetic allometry accounts for a large proportion of shape variability in our sample.

A further examination of Figure 7 points to one other interesting finding; in terms of size and shape variability along PC I it appears that adult females are at least in part, allometric equivalents of males. The principal shape differences between the adults of each sex on this PC seem to be explained by ontogenetic allometry (but see findings in relation to PC II, below).

Principal component I effectively represents a good linear allometric model of ontogenetic shape change in the face of *Cercocebus torquatus*. We examine the allometric model in greater detail below through the

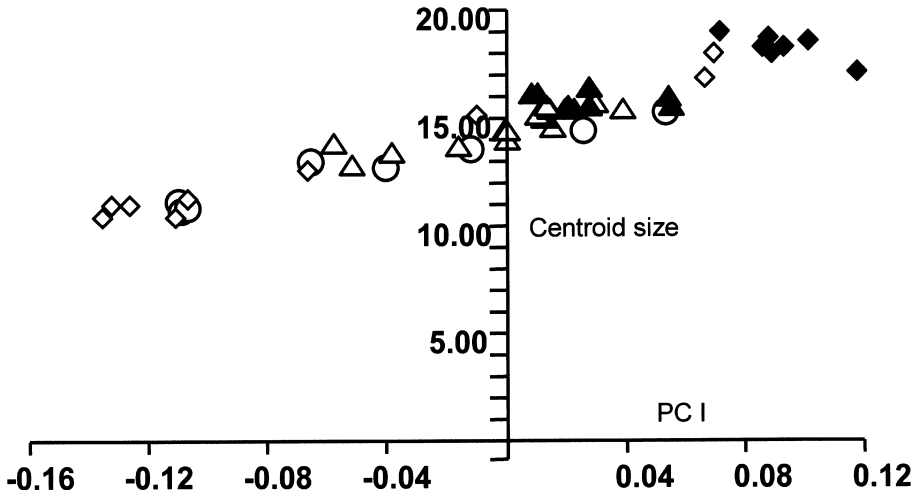

Fig. 7. Plot of the first principal component (horizontal axis) from PCAt vs centroid size (cm) for the whole sample. Diamonds, males; triangles, females; circles, sex unknown; black markers, adults.

'morphing' of a mean individual. One issue that we cannot address is that of the timing of growth since no data are available on age at death for our sample. It is possible to make some rough estimate of age based on patterns of dental eruption but the timing of eruptions is only a crude estimator and may differ between males and females (as in macaques; Richtsmeier et al. 1993*b*). We cannot therefore assess whether males achieve adult morphology through an extended or accelerated ontogeny. Likewise we are unable to determine if the relationship between centroid size and age is linear or nonlinear. As such no conclusions can be drawn about the temporal pattern of changes in size and shape or about time vs rate hypermorphosis in males relative to females.

PC II (Fig. 6) shows no ordering of specimens with respect to age. Subadult males and females overlap considerably but adult males appear separate from adult females. A t test carried out on the scores of adult males and adult females on PC II indicates that the difference between the means of adults of each is highly significant ($P < 0.003$). This indicates that a significant aspect of the difference in shape between adult males and females is not explained by the growth allometry modelled by PC I. Thus the dashed lines drawn over Figure 6, such that they encompass the limits of sample variation on PC II, diverge towards the right (in the region of adults) indicating that greater differences exist on PC II amongst older than younger specimens. This divergence coincides with the appearance of sexual dimorphism on PC II in older and adult specimens. It appears, therefore, that some aspects of sexual dimorphism in facial shape are not explained by hypermorphosis in males relative to females, rather growth allometries diverge between the sexes immediately before they achieve maturity. The higher PCs (PC III and above) show no evidence of sexual dimorphism or size related variation.

Visualisation of allometry

'Morphing' the mean. Having discovered the presence of an interesting allometry in PC I we next turn to visualisation. By visualising shape differences we can hope to achieve some deeper understanding of the nature of this allometry. The visualisation technique we adopt in this study relates variation along any chosen PC to a deformation of the mean shape. Thus we take the mean shape and deform it such that it comes to adopt the shape with score 0 on all PCs except the one we are investigating. In Figure 8 we present 3 representations of the mean shape. The wireframe model *A* is concise and allows us to readily illustrate boundaries between bones but it is less visually appealing than the flat surface rendered model, *B*, in which triangles define surfaces between landmarks such that they connect to form a reasonable representation of a face. The smooth rendered model, *C*, is achieved through Gouraud shading which 'smoothes' edges. This image is more visually appealing although the loss of edges can be confusing if we are concerned to interpret shape transformations in terms of the landmarks defining the edges.

The simplest way of visualising variation along PC I is to use the animation features of our software suite to morph the mean shape along it. This is very informative but for presentation in this paper still images are required. We have therefore prepared Figure 9 such that, from left to right, we present smooth rendered and wire frame images of the warped

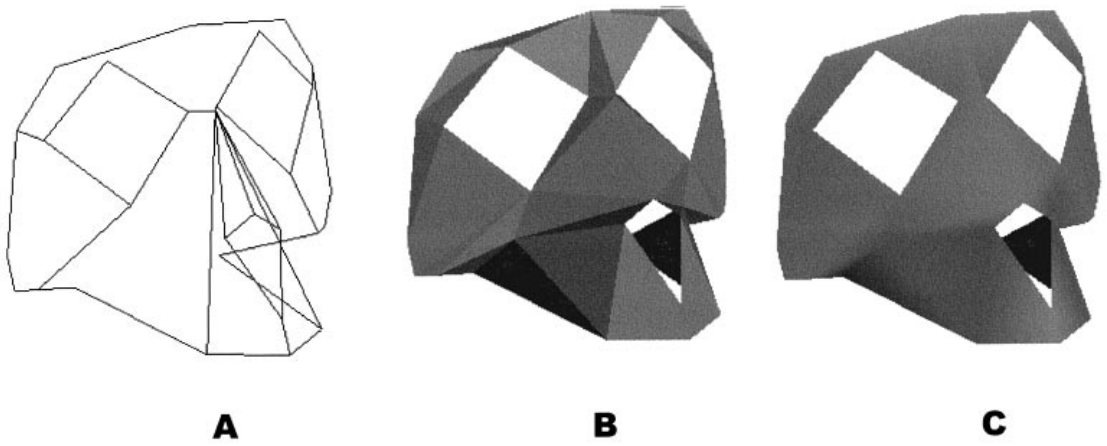

Fig. 8. Mean face. (*A*) Wireframe approximately delineating sutural boundaries. (*B*) Flat surface rendering. (*C*) Smooth surface rendering.

mean at the extremes and middle of PC I. In a sense each of these images represents the mean, the leftmost the mean shape for small specimens (score on PC I of -0.12), the middle, the overall mean (PC I = 0.0) and the rightmost the mean shape for large specimens (PC I = 0.12). We have already determined that this PC represents ontogenetic allometry and some aspects of sexual dimorphism and so this series of images represents the changes in shape which occur during growth and rightmost pair of images gives us an indication of a component of the sexual shape differences between adults.

The shape differences between these images suggest that as scores on PC I increase the maxillae and premaxillae become prognathous and the midface relatively larger with respect to the orbits. Other differences in proportion between regions are best appreciated from the wireframe reconstructions in the upper row of Figure 9. Readily apparent are changes in the proportionate size and shape of the premaxilla which is relatively larger and broader in small individuals (low score on PC I) than in older. The maxilla shows a marked increase in relative antero-posterior length and height, the nasal aperture and orbits become relatively smaller and the bridge of the nose relatively larger. Note that the shape differences are a composite of uniform and nonuniform 'stretchings' although they are described by a simple linear equation, that of the first principal component. This may be surprising at first but remember the model is linear because the pattern of shape change is consistent throughout ontogeny, not because the shape change is simple.

Cartesian transformation grids. An alternative visualisation technique is based on the cartesian transformation grids of Thompson (1917). Thomson's proposal was that a deformed grid drawn over the target specimens represents differences in form. The deformation of the grid effectively indicates a deformation of the space in the vicinity of the reference form that takes every feature in this form into its homologue in the target. Cartesian transformation grids of this type provide an intuitively interpretable static representation of shape differences. The application of transformation grids in this study is illustrated in Figure 10. In this diagram the left hand frame, *A*, represents the mean shape with a score of -0.12 (small centroid size), the right hand frame, *B*, represents the mean shape with a score on PC I of 0.12 (large centroid size; see Fig. 9). A regular, square grid, representing a slice of the space in the vicinity of *A* is drawn over it and a deformed grid occupies the equivalent space over *B*. The deformation of this grid represents the deformation of this slice of space when landmarks in A are mapped into their equivalents in *B*. The grid is drawn using the thin plate spline (Bookstein, 1989) and, as such, its deformation is minimised in terms of the bending energy of this spline which is a measure of nonuniform bending. This is an eminently reasonable basis for calculation of the grid but bear in mind that it represents one of many possible mathematical models of deformation (minimum bending) rather than any specific biological one.

The transformation grid can be drawn as a cubic grid in 3 dimensions but interpretation is confusing since many crossing lines in many planes are drawn at once. In our implementation we choose instead to draw the grid in 1 of 3 planes which can be moved through the volume of the target or reference image. As the sections float through the image the grids representing them deform in 3 dimensions and these

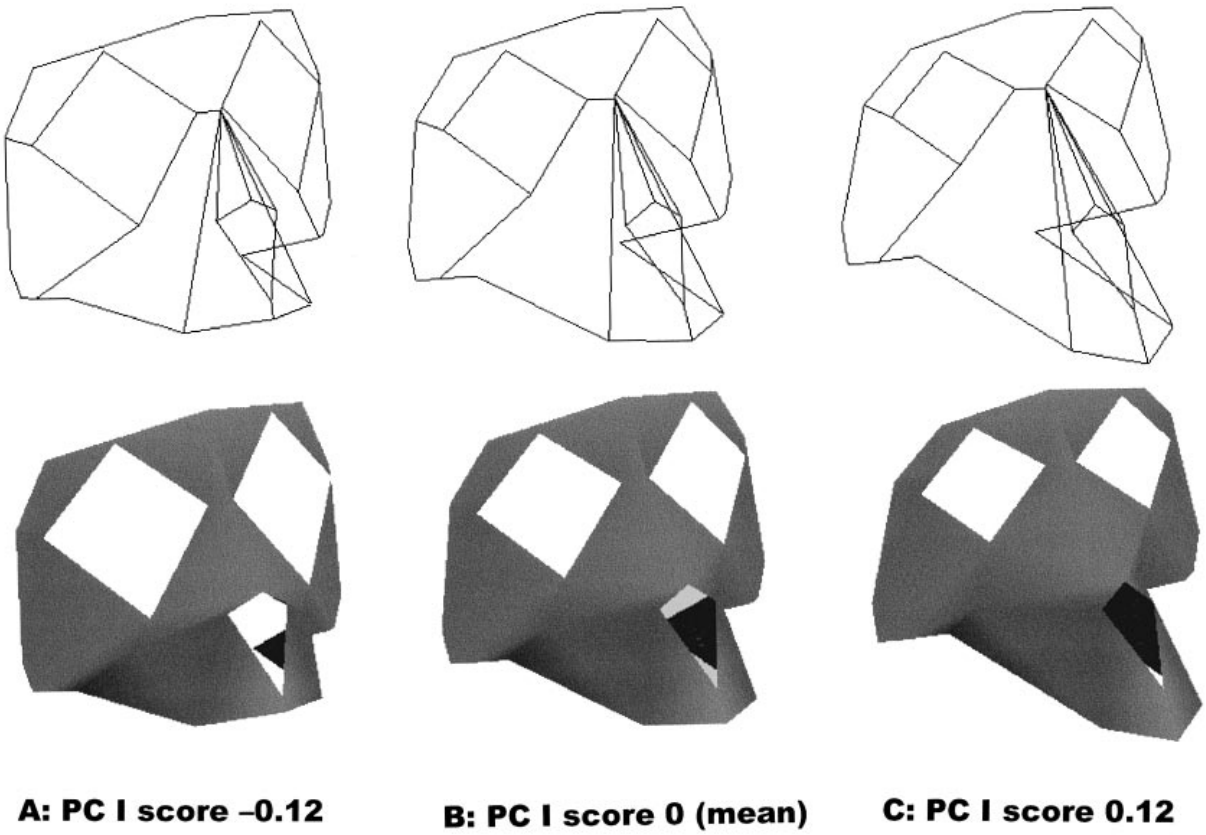

Fig. 9. Variation in shape represented by PC I. Top row, wireframe images, bottom row smooth rendered. From left to right each column shows the mean shape for the sample with scores on PC1 of −0.12, 0 and 0.12 respectively.

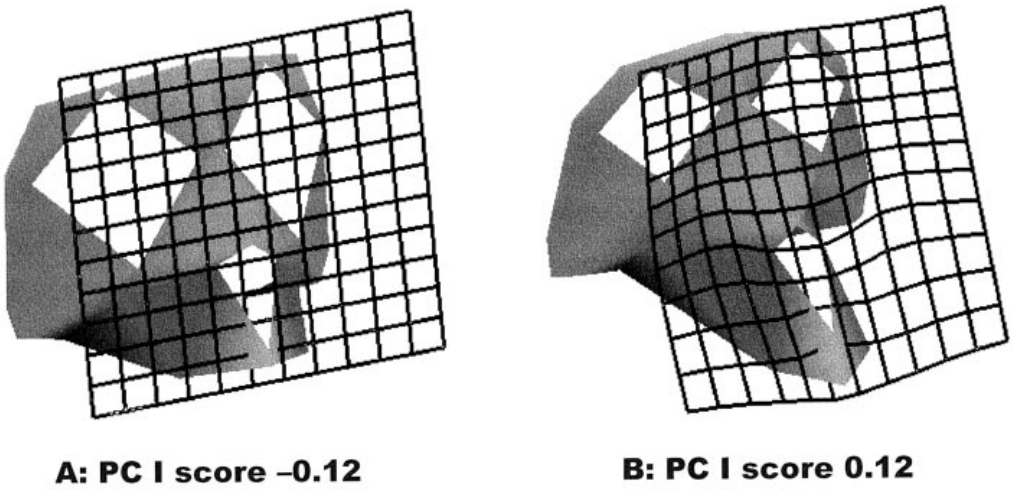

Fig. 10. Shape variation along PC I visualised with a transformation grid calculated using a triplet of thin plate splines. (*A*) A square grid in the vicinity of the shape represented by a score of −0.12 on the first principal component and 0.0 on all other PCs is deformed in (*B*), such that displacements of its nodes indicate the relative deformation of this slice of space required to map all landmarks in *A* to those in *B*.

deformations allow us to visually appraise localised and more global shape differences.

In Figure 11 we present a series of 6 images representing the deformation between 'small' and 'large' (PC I score of −0.12 and 0.12, all other PCs score 0.0) mean forms illustrated in Figure 11. Transformation grids are drawn on these in coronal (*A*, *B*, *C*, *E*), horizontal (*D*) and sagittal (*F*) planes in order to facilitate interpretation of the shape differences between the extremes of PC I (and given

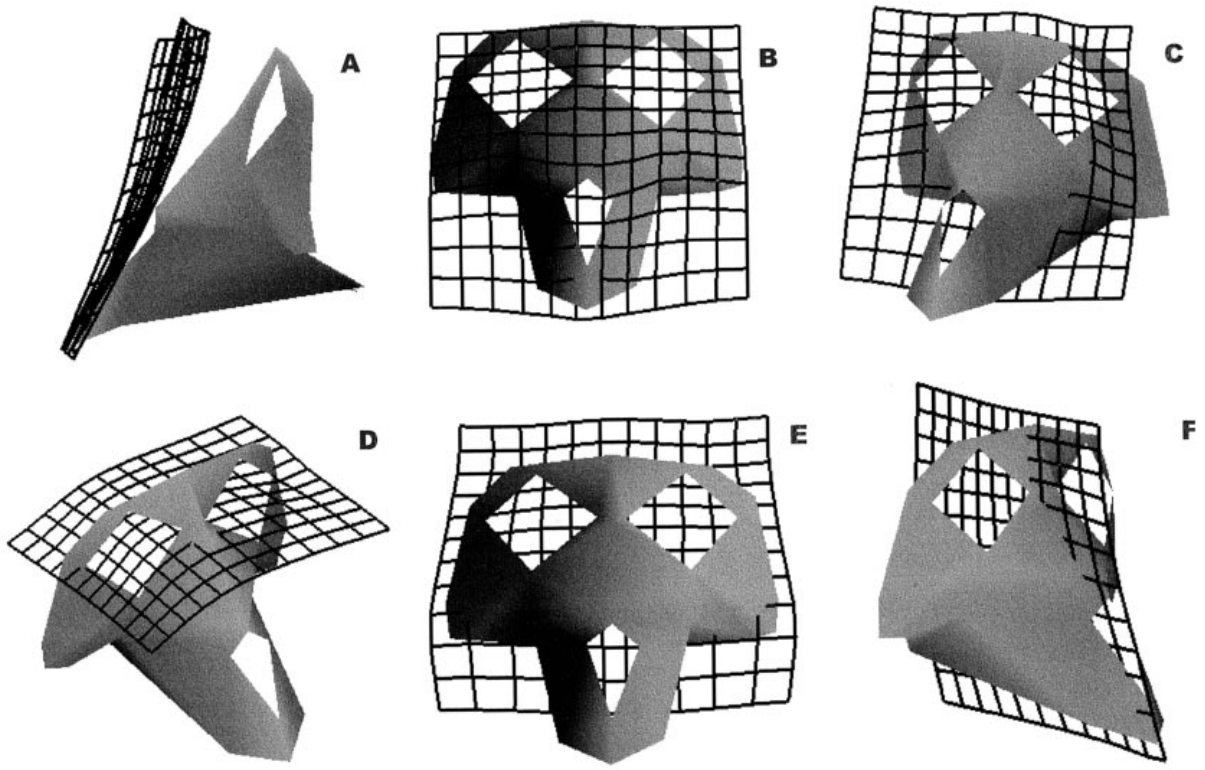

Fig. 11. Transformation grids calculated using a triplet of thin plate splines derived from the difference between reference form (PC I score of −0.12, score of 0.0 on all other PCs) and target form (PC I score 0.12, 0.0 on all other PCs). The transformation grids are drawn in varied locations and planes in the space of the target form. See text for discussion.

the high correlation, size). Frames *A* and *B* in Figure 11 show a transformation grid placed such that its most inferior part lies just within the anterior premaxilla. In the reference form this grid is vertically placed (see Fig. 10*A*) in the target the grid is curved gently posterosuperiorly and transversely (Fig. 11*B* and *A*). This curvature reflects the considerable relative anterior displacement of the subnasal region that accompanies increased prognathism with increasing size. This is also shown very clearly by the deformation of the sagittally placed grid in Figure 11*F*.

More subtle deformations are seen in Figure 11*B*. The horizontal grid lines just anterior to the upper part of the nasal aperture are deflected inferiorly indicating a relative downward displacement of this region together with a relative expansion of the nasal bridge. The vertical grid lines passing through the subnasal region become less widely spaced in the midline indicating a relative narrowing. The horizontal lines in this region indicate relative expansion in height of the subnasal region and relative downward displacement of the upper nasal aperture, a relative contraction in height of the nasal aperture. Although the grid of Figure 11*B* shows some medial bending of the vertical lines which pass over the nasal aperture, this bending is less than that of the horizontal lines indicating that the nose becomes relatively smaller in height than it does in width. A similar deformation is seen in the region of the orbits in Figure 11*C*. This grid, drawn such that it passes through the orbital planes, shows a relative decrease in height with respect to width in the region of the orbits. The grid of Figure 11*D* indicates that this change in orbital proportions is accompanied by a relative dorsal displacement of the orbital region (which reflects prognathism rather than any movement with respect to the cranial base).

The grid of Figure 11*C* also indicates a marked relative expansion and posterior migration of the maxillary fossae, just as the grid lines pass through the rendered surface. Other changes in the region of the zygomatic are shown in Figure 11*E* in which a transverse grid is drawn through the plane of the zygomatic roots. Laterally, the grid becomes expanded in the zygomatic region, indicating a relative increase in breadth of this region with growth.

Figure 12 illustrates shape variability along PC II, which significantly separates adult males from adult females (but not infants or juveniles of either sex). Figure 12*A* shows a hypothetical specimen with a score of 0.06 on PC II and 0 on all other PCs. Figure 12*B*

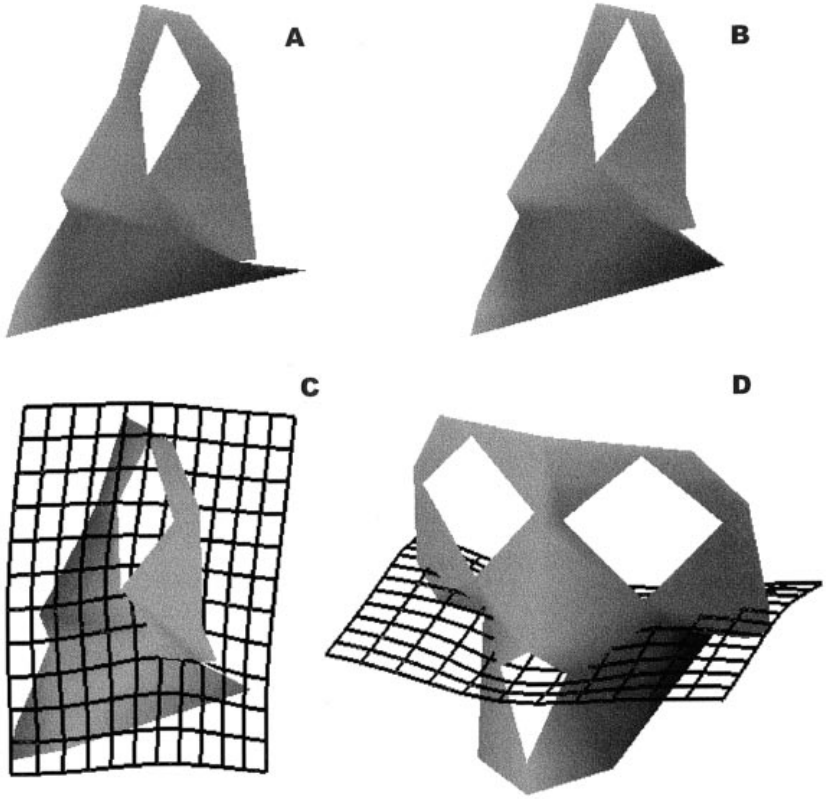

Fig. 12. Variation along PC II. The upper 2 images show the mean shape morphed to the extremes of PC II. Upper left, score on PC II of 0.06; upper right, score on PC II of −0.06. The transformation between upper left and upper right images is visualised by means of cartesian transformation grids in the lower 2 images. Although the shape which is being morphed represents the overall mean we can read the transformation grids as an exaggerated (by an approximate factor of 2) representation of the apparent differences between adult female and adult male means on this axis.

represents a score at the other extreme (score −0.06) of PC II. Figure 12*C* and *D* shows grids indicating the transformation from Figure 12*A* to Figure 12*B*. From these it appears that PC II captures sample variability in the set of the midface with respect to the upper face. In Figure 12*C* the grid is drawn just lateral to the muzzle and it shows a distinct kink such that the midface appears to swing under the orbital region with the axis for this rotation passing through the maxillary fossae. Figure 12*D* illustrates that this swinging under of the midface results in a relative downward rotation of the upper nasal region with respect to the lower orbital.

Given that males have lower scores on PC II than females, these diagrams indicate that males have a different set of the midface with respect to the upper face compared with females, male muzzles being relatively rotated under the upper face. This is accompanied by a relative downward rotation of the upper nasal region with respect to the lower orbital. Note, however that the range of scores on PC II represented in Figure 12 is approximately twice the difference in scores between male and female adult means so the impression of difference between adults of each sex on this axis is exaggerated by a factor of 2. The variation along PC II may also be significant with respect to interpreting the significance of the large resorptive area in the maxillary fossae since this region seems to incorporate the axis of rotation about which the set of the midface varies with respect to the upper.

Summary of results

Tests of technique indicate that errors of precision of measurement were small compared to the variability of the same as a whole. Furthermore no appreciable difference was found between the results of PCA and PCAt and we take this to indicate adequate concentration of data since our results are robust in the face of different projections.

The PCAt of our sample results in a first principal component that accounts for 52% of the total variance. Unique amongst PCs, PC I shows 2 biologically interesting correlations. First centroid size correlates 0.95, $P < 0.001$, with scores on PC I

and second, adult males and females are completely separated indicating that a proportion of the sexual dimorphism in face shape in this species is identical to ontogenetic scaling.

We visualise the geometry of shape variation along PC I using rendered reconstructions of the mean at the extremes of PC I and cartesian transformation grids. These allow us to conclude that the differences in face shape between small and large ($\sim$ young and old) and a component of that between female and male adults includes increasing prognathism involving maxillae and premaxillae, relative lengthening of the maxillary alveolar border and increase in maxillary height, relative shortening and narrowing of the premaxilla, relative contraction of the subnasal region and, together with relative downward displacement of the upper nasal aperture, relative contraction in height of the nasal aperture, relative decrease in height with respect to width of the orbits accompanied by a relative dorsal displacement of the orbital region and a marked relative expansion in the region of the maxillary fossae accompanied by a relative posterior displacement of the maxillary fossae and lateral expansion of the zygomatic region.

Scores on PC II are independent of the growth allometry of PC I but are related to adult sexual dimorphism. The principal aspect of variation represented by PC II is the set of the upper face with respect to the midface and the axis about which these rotate relative to each other passes through the maxillary fossae; the location of a large and consistent resorptive field. The significant difference between adult males and females on PC II indicates that the sexes diverge in growth allometry immediately before achieving maturity.

DISCUSSION

Ontogenetic allometries: remodelling and bone displacement during growth

The relationship between cortical remodelling activity and bone displacements is difficult to examine although it is currently hypothesised that the former to a large extent compensates for the latter during growth to maintain functional alignment (Enlow, 1968, 1975).

In order to test this hypothesised link between remodelling and displacement we would ideally characterise both and look for correlations between them. This kind of analysis is not possible, however, because of the interweaving of these processes during growth. Growth at sutures will lead to bone displacement but depository activity at the tips of bones will also lead to the impression of displacement. In addition it is impossible to say what bone is being displaced where in the absence of registration points; we will always end up saying that bones move relative to some other bones and this will inevitably introduce major complications in understanding the whole.

In this study, the landmarks indicate equivalent points of various types. Some part of their variation in location is due to displacement but it is likely that remodelling activity also plays a part. Thus the relative posterior displacement of the maxillary fossa can probably be attributed mainly to the large consistent resorptive field found in this location. In contrast, the changes in the subnasal region are more likely to come about through differential deposition on surfaces and at sutures. Our morphometric analysis therefore embodies both aspects of facial growth to some degree.

We cannot directly separate the contributions to growth made by remodelling and displacement; instead we will have to be content with comparing overall growth vectors and remodelling maps between species in the expectation that we will be able to draw sensible conclusions and build useful analytical models and frameworks. If remodelling activity appears fairly constant in type, location and degree throughout ontogeny can we infer that overall ontogenetic allometries (which arise through displacements and compensatory remodelling) are also constant? The hypothesis under test is therefore a modified version of Enlow's: that consistency of remodelling activity indicates consistency of ontogenetic allometries.

Earlier studies of facial remodelling in *Cercocebus torquatus atys* (O'Higgins et al. 1991) demonstrated that the locations of depository, resorptive and resting surfaces on the external surfaces of the facial skeleton remain more or less constant throughout growth between completion of the deciduous dentition and appearance of M3 (Fig. 1). Active deposition is observed over most of the face including particularly the subnasal region, maxillary alveolus and superior and lateral orbital margins. Large and constant resorptive fields are observed over the maxillary fossae although their relative size diminishes with growth. In the oldest individual examined a small resorptive field is apparent medial to the orbits over the lateral aspect of the bridge of the nose. This consistency of location and type of remodelling activity was interpreted by O'Higgins et al. (1991) to indicate a consistent postnatal growth allometry in the face of this species during the examined growth

range. This interpretation was, however, based on the assumption that remodelling activity can be used as an indicator of bone displacements, the former being compensatory for the latter in maintaining functional alignment during growth. This study provides us with an opportunity to test this earlier conclusion and so, indirectly, to test Enlow's (1975) hypothesis that bone growth remodelling is to a large extent compensatory for displacement.

An earlier attempt at examining facial growth in this species using geometric morphometric tools was reported by O'Higgins & Dryden (1992). At the time of this earlier study many issues surrounding registration, shape spaces, and tangent spaces were still unresolved; as a consequence the methods applied were relatively simple. 2D cartesian transformation grids were calculated between midline landmark coordinates from pairs of specimens of different ages. The general conclusion from that study was that, overall, growth allometries appeared stable postnatally although there were some apparent differences in growth vectors from age group to age group. With our more sophisticated analysis in this study we are able to conclude that these differences were probably artifactual and due to sampling error.

In this paper we are able to revisit this question of growth allometry with a comprehensive battery of 3D tools for analysing shape variability. Our findings are that a single linear model, in the form of PC I, almost completely explains size-related shape change during the growth of the face of *Cercocebus torquatus* between completion of deciduous dentition and the appearance of M3. One principal allometric trend emerges and this is consistent throughout the size range we have studied. We conclude that remodelling and displacement are more or less constant in location and type.

This finding fails to falsify the broad hypothesis that consistency of remodelling activity indicates consistency of ontogenetic allometries. If this finding is repeated in studies of other species then we may well be able to use remodelling maps from a single individual to infer something of ontogenetic allometries for the species. The relationship between growth remodelling and growth allometry may, however, be fairly loose. It may be that small differences in growth allometries are accommodated by subtle adjustments in the rates of remodelling in established fields (which cannot easily be discovered through SEM studies) new ones appearing only when rate changes are inadequate to compensate. Further studies are called for to clarify this issue.

Growth allometries appear to diverge between the sexes just before they achieve maturity. The remodelling maps of Figure 1, do not include specimens with adult canines and M3s. The oldest specimen does, however, manifest a resorptive field over the lateral aspect of the bridge of the nose. It may be that this is indicative of divergence of facial growth in older individuals from the pattern seen in younger specimens. Further remodelling studies of older specimens are required to confirm or deny this.

Our present knowledge of remodelling maps leads us to suggest cautiously that knowledge of remodelling activity might be turned to the reconstruction of broad rather than specific ontogenetic allometries in extinct species. More, detailed studies are called for to explore this possibility and the limits of any such inference.

Ontogenetic allometries: the geometric growth model

Besides an analysis and visualisation of growth allometries in relation to growth remodelling, our study has resulted in a statistical model of facial growth allometry in *Cercocebus torquatus*. It allows us to conclude that, in this species, there is a linear relationship between size and shape of the face. We have already noted that this does not necessarily imply a linear relationship between age and shape since size and age may not be linearly related in either or both sexes.

Further studies will address age, size and shape but for now we have a useful model which we might turn to other uses. Our model is such that it will allow a quantitative comparison of the overall growth allometry in this species with that in any other. Growth allometries might be compared in terms of the angles between principal components and visualised in terms of PC plots and the differences in growth. The growth model also allows 'prediction' such that any specimen can be 'grown' (morphed) up or down the growth allometry in order to estimate its adult or infant shape. We have carried out such an analysis for the mean shape in this study but the application of this technique to fossil specimens might well turn out to be of interest in understanding the ontogenetic basis of phylogenetic transformations. Further, the application of this approach to forensic reconstruction and medical growth prediction is also worth exploring in future work.

Ontogenetic allometries: comparisons with other monkeys

Using FESA and/or EDMA, Richtsmeier and colleagues have examined growth in several monkey

species. In the face of *Cebus apella* (Corner & Richtsmeier, 1991) both males and females show anterolateral growth around the lateral and inferior rim of the orbit and a generalised growth of the muzzle along the anteroposterior axis. Males and females show similar growth patterns with males tending to be larger than females at equivalent growth stages ($\sim$ ages). In *Saimiri sciereus* (Corner & Richtsmeier, 1992) growth across the orbits is small although the lateral part of the orbit shows substantial growth along the anteroposterior axis. In the midface, the anterior parts grow mainly downwards and forwards relative to the neurocranium and the posterior parts along an axis orientated postero-inferior to anterosuperior. Sexual dimorphism is minimal in this species and this is reflected in a similar growth pattern between sexes with males extending it a little through an extended period of growth (time hypermorphosis). Growth of the face in *Ateles geoffroyi* (Corner & Richtsmeier, 1993) is characterised by an early expansion of the nasopharyngeal region followed by later anterior projection of the lateral zygoma and advancement local to the premaxilla. Sexual dimorphism is very slight in this species although there is an indication of an earlier completion of female relative to male facial growth. In *Macaca fascicularis* (Richtsmeier et al. 1993*a*) growth is most pronounced in the muzzle; it grows forwards and vertically in height whilst the premaxilla rotates downwards and lengthens along its alveolar border. The region of the zygoma shows lateral flaring of its inferolateral aspect and the orbits change little.

In all these studies Richtsmeier and her colleagues have focused on differences in form between successive age groups. This approach leads them to identify subtle differences in growth patterns from one pair of age group comparisons to the next. Against these differences should be set our finding of a generally consistent pattern of size-related shape change throughout the postnatal period in *Cercocebus torquatus*. This finding contrasts with earlier indications (O'Higgins & Dryden, 1992) from less secure analyses that there may have been subtle differences in ontogenetic allometry from age group to age group.

Richtsmeier et al. (1993*b*) carried out a study to compare growth patterns between 3 monkey species (*Macaca fascicularis*, *Cercopithecus aethiops* and *Cebus apella*). In order to compare patterns of growth they extended the methods of EDMA to compute growth difference matrices. Their findings indicate that differences between adult forms are due in part to differences in natal morphology and in part to differences in growth vectors. Our approach, PCA of coordinate data, also enables comparisons of growth vectors and we hope to extend our methods to allow the growth model from one species to be applied to another (as modifications of EDMA also do). This type of 'growth experiment' may have particularly interesting applications in the study of fossils.

Remodelling maps are known for the faces of a few individuals from a few species of primates; the relevant studies are cited in the Introduction. The only other Old World monkey studied in detail is the rhesus macaque (Enlow, 1966) and in this species the remodelling map is very similar to that of *Cercocebus torquatus*. In *Macaca fascicularis* (Richtsmeier et al. 1993*a*) forward and vertical growth in the muzzle is pronounced and the premaxilla rotates downwards and lengthens along its alveolar border. The inferolateral aspect of the zygomatic bone shows lateral flaring whilst the orbits show little shape change. This description is similar to our findings for *Cercocebus torquatus*. It suggests that macaques and mangabeys, which show similar remodelling patterns in the face, also have similar growth vectors. We have, however, observed in the sooty mangabey, an allometric change in orbital proportions and, in this species, downward rotation of the premaxilla is a mode of variation shown by PC II rather than by the allometric component, PC I.

The 'common' pattern of remodelling in macaques and mangabeys differs from that found in a single specimen of *Ateles geoffroyi* in which there is much more limited resorption over the maxilla (unpublished study by the principal author). Corner & Richtsmeier's (1993) description of growth in the face of this species also indicates differences from macaques and mangabeys. From these comparisons it appears that general similarity of remodelling activity may well indicate similarity in general growth vectors in the face but more specific differences in growth vector are accommodated by subtle differences in remodelling rates not readily appreciated through microscopy. This conclusion requires further testing through the comparison of remodelling maps and statistical growth models across a wider range of species.

Sexual dimorphism

We have already noted that PC I accounts for a proportion of the differences in shape between the sexes in adults. Additionally, a *t* test indicates a highly significant ($P < 0.003$) difference between the means

of adult males and females on PC II. Visualisation of variations on PC II indicates that the differences in shape accounted for by this PC are principally related to the set of the midface with respect to the upper face.

The sexual differences on PC I indicate that, in part, sexual dimorphism in the face of *Cercocebus torquatus* is explicable in terms of ontogenetic scaling males being allometric equivalents of females. However the findings with respect to PC II indicate that as maturity is achieved there is a divergence of growth allometry between the sexes. Thus, we falsify the second of our initial hypotheses: that the ontogenetic allometries of males and females are identical.

This finding is consistent with sexual dimorphism in the face of this species being due in part either to a rate or time hypermorphosis (Shea, 1983, 1986) in males relative to females. In the absence of data on absolute ages we are unable to distinguish between these possibilities.

Ontogenetic scaling is also noted between the sexes of *Cebus apella* (Corner & Richtsmeier, 1991), *Saimiri sciureus* (Corner & Richtsmeier, 1992) and *Macaca fascicularis* (Richtsmeier et al. 1993*a*). The mechanism of ontogenetic scaling varies amongst these species, in *Cebus apella* rate hypermorphosis predominates, in *Saimiri sciureus* time hypermorphosis is dominant and in the macaque, rate and time hypermorphosis both operate.

Analytical approach

We have used tools from geometric morphometrics (Marcus et al. 1996) to examine growth and sexual dimorphism in the face of the sooty mangabey. Our implementation is designed to facilitate interactive exploration of shape variation and to produce graphical output suitable for publication. By and large this interactive aspect allows ready appreciation of the relationship between shape variability and PC scores although the cartesian transformation grids provide useful static representations of the same changes.

Whilst such visualisations are in themselves interesting it can be argued that the insights they produce are more or less consistent with the conclusions that could be drawn from careful visual appraisal. This is doubtless true, although quantitative estimation of the mean shape at any particular size is likely to minimise errors of judgement. Major benefits of the quantitative approach are that the pattern of growth is statistically modelled, that the resultant growth models can be statistically compared between species and that they can be turned to prediction of adult shape from juveniles and vice versa.

The use of PCA in allometric studies is well established for log transformed interlandmark distances (Jolicoeur, 1963). In dealing with interlandmark distances (ilds), size and shape differences are usually treated simultaneously (no prescaling) and as such the first PC often reflects size differences, eigenvectors for this PC being equivalent to classic allometric coefficients (exponents) when data are logged. We are unaware of any growth study that has used sufficient ilds to allow full geometric reconstruction (up to reflections) of the forms under analysis but intend to explore this approach in a future study.

There are important statistical issues remaining to be resolved with respect to the best choice of method of analysis – EDMA, PCA of ilds or of Procrustes registered coordinates (see Lele, 1993; Rao & Suryawanshi, 1996; Dryden & Mardia, 1998). Some argue for one method over another but in the absence of statistical agreement we advocate pragmatism. If the biological phenomenon we are studying has large effect relative to the differences resulting from choice of method (as should be the case in sensible analyses) all methods will lead to nearly identical biological conclusions. We intend to pursue this issue in a further empirical study of the consequences of method choice.

Note that in PCA of ilds for the study of allometry, data are logged partly because the expectation is that size/shape relationships will be exponential and pass through the origin. In the context of landmark analyses, however, logging makes no sense and so we analyse registered raw coordinates. Our findings indicate that over the size range studied size/shape relationships are linear in this sample (at least up to eruption of M3 and canines, after which PC II shows an interesting difference between sexes). In other species non-linearity might show a more marked curved allometry encompassing 2 or more PCs and in such cases scores on these PCs could be incorporated into a more sophisticated model of allometry.

CONCLUSIONS

This study has demonstrated the viability and potential of using geometric morphometric approaches in studies of 3-dimensional growth of the face. It has failed to falsify the hypothesis that consistency of remodelling activity indicates consistency of ontogenetic allometries (modified from Enlow, 1968,

1975). It has, however, falsified the hypothesis that the ontogenetic allometries of males and females of *Cercocebus torquatus* are identical; instead it appears that differences between the sexes arise in part through ontogenetic scaling and in part through divergence of growth allometry between the sexes just before maturity.

ACKNOWLEDGEMENTS

We could not have begun this work without the support of our statistical colleagues; Professor Kanti Mardia, Dr Ian Dryden and Professor John Kent of the Department of Statistics, University of Leeds. They have always been enthusiastic in providing help and in explaining with the most difficult mathematical concepts. Ian Dryden has been especially supportive in helping P.O'H. to programme the tangent space projection and verify its functioning. The Leeds group provided the basic algorithm for the computation of the thin plate splines and cartesian transformation grids. Other, much more statistically knowledgeable workers than the authors have also contributed valuable advice in the construction of our programme suite. These include Dr Fred Bookstein (Michigan), to whom we are grateful for introducing the thin plate spline and its more exotic variants to morphometrics, Dr Les Marcus (New York) for common sense advice in the face of multiple choices and Dr Subhash Lele for stirring the pot, introducing caution and making us think very hard about what we were doing.

The programming that underpins this study has made demands on the patience of our colleagues Professor Christopher Dean and Dr Fred Spoor. We are grateful for their understanding and also for the many useful comments they have made at every stage of this work. Nicholas Archibald has been closely associated with the development of our software and the many questions he has asked have helped to clarify otherwise ignored issues. Una Strand Vidarsdottir put great effort into the setting up of our digitiser and together with Sam Cobb was enormously helpful in ensuring our data were gathered well. Gary Schwartz, Christopher Dean and Ian Dryden made helpful comments on an earlier draft of this paper but any errors that remain are ours alone.

The remodelling maps for sooty mangabeys would never have been made without the enthusiastic input of Dr Tim Bromage (CUNY, New York). He not only shared his valuable knowledge and techniques but also asked sufficient difficult questions to set the work leading to this paper in motion. We thank the Natural History Museum, London and especially Paula Jenkins for granting access to the collection of primate material. This manuscript is much improved following the comments of 3 anonymous referees.

REFERENCES

Bookstein FL (1978) *The Measurement of Biological Shape and Shape Change. Lecture Notes in Biomathematics*. New York: Springer.

Bookstein FL (1987) On the cephalometrics of skeletal change. *American Journal of Orthodontics* **83**, 177–182.

Bookstein FL (1989) Principal warps: thin-plate splines and the decomposition of deformations. *IEEE Transactions in Pattern Analysis and Machine Intelligence* **11**, 567–585.

Boyde, A, Jones SJ (1972) Scanning electron microscopic studies of the formation of mineralised tissues. In *Developmental Aspects of Oral Biology* (ed. Slavkin HC, Baveta LA), pp. 243–274. New York: Academic Press.

Bromage TG (1986) *A comparative scanning electron microscope study of facial growth remodelling in early hominids*. PhD thesis: University of Toronto.

Cheverud J, Lewis J, Bacharach W (1983) The measurement of form and variation in form: an application of three-dimensional quantitative morphology by finite-element methods. *American Journal of Physical Anthropology* **62**, 151–165.

Cheverud JM, Richtsmeier JT (1986) Finite element scaling techniques applied to sexual dimorphism in rhesus macaque (*Macaca mulatta*) facial growth. *Systematic Zoology* **35**, 381–399.

Corner BD, Richtsmeier JT (1991) Morphometric analysis of craniofacial growth in *Cebus apella*. *American Journal of Physical Anthropology* **84**, 323–342.

Corner BD, Richtsmeier JT (1992) Morphometric analysis of craniofacial growth in the squirrel monkey (*Saimiri sciureus*): a quantitative analysis using three dimensional coordinate data. *American Journal of Physical Anthropology* **87**, 67–82.

Corner BD, Richtsmeier, JT (1993) Cranial growth and growth dimorphism in *Ateles geoffroyi*. *American Journal of Physical Anthropology* **92**, 371–394.

Dryden IL, Mardia KV (1993) Multivariate shape analysis. *Sankya* **55(A)**, 460–480.

Dryden IL, Mardia KV. (1998) *Statistical Shape Analysis*. London: John Wiley, in press.

Enlow DH (1966) A comparative study of facial growth in *Homo* and *Macaca*. *American Journal of Physical Anthropology* **24**, 293–308.

Enlow DH (1968) *The Human Face: An Account of the Postnatal Growth and Development of the Craniofacial Skeleton*. New York: Harper and Row.

Enlow DH (1975) *Handbook of Facial Growth*. Toronto: W.B. Saunders.

Gower JC (1975) Generalised Procrustes analysis. *Psychometrika* **40**, 33–50.

Goodall CR (1991) Procrustes methods and the statistical analysis of shape (with discussion), *Journal of the Royal Statistical Society Series B*, **53**, 285–340.

Jolicouer P (1963) The multivariate generalisation of the allometry equation. *Biometrics* **19**, 497–499.

Johnson PA, Atkinson PJ, Moore WJ (1976) The development and structure of the chimpanzee mandible. *Journal of the Royal Statistical Society Series B* **56**, 285–299.

Kendall DG (1984) Shape manifolds, Procrustean metrics and complex projective spaces. *Bulletin of the London Mathematical Society* **16**, 81–121.

Kent JT (1994) The complex Bingham distribution and shape analysis. *Journal of the Royal Statistical Society Series* B **56**, 285–299.

Krogman WM (1974) Craniofacial growth and development: an appraisal. *Yearbook of Physical Anthropology* **18**, 31–64.

Le H, Kendall DG (1993) The Riemannian structure of Euclidean shape spaces. A novel environment for statistics. *Annals of Statistics* **21**, 1225–1271.

Leigh SR, Cheverud JM (1991) Sexual dimorphism in the baboon facial skeleton. *American Journal of Physical Anthropology* **84**, 193–208.

Lele S (1993) Euclidean distance matrix analysis: estimation of mean form and form difference. *Mathematical Geolology* **25**, 573–602.

Marcus LF, Corti M, Loy A, Naylor GJP, Slice D (eds) (1996) *Advances in Morphometrics*. New York: Plenum Press.

Moss ML, Young RW (1960) A functional approach to craniology. *American Journal of Physical Anthropology* **18**, 281–292.

O'Higgins P (1997) Methodological issues in the description of forms. In *Fourier Descriptors and their Applications in Biology* (ed. Lestrel PE), pp. 74–105. Cambridge: Cambridge University Press.

O'Higgins P, Moore WJ, Johnson DR, McAndrew TJ, Flinn RM (1990) Patterns of cranial sexual dimorphism in certain groups of extant hominoids. *Journal of Zoology*, *London* **222**, 399–420.

O'Higgins P, Bromage TG, Johnson DR, Moore WJ, McPhie P (1991) A study of facial growth in the sooty mangabey *Cercocebus torquatus*. *Folia Primatologica* **56**, 86–94.

O'Higgins P, Dryden IL (1992) Studies of craniofacial growth and development. *Perspectives in Human Biology* **2**, *Archaeology in Oceania* **27**, 5–104.

Rao CR , Suryawanshi S (1996) Statistical analysis of shape of objects based on landmark data. *Proceedings of the National Academy of Science of the USA* **93**, 12132–12136.

Richtsmeier JT (1989) Applications of finite-element scaling analysis in primatology. *Folia Primatologica* **53**, 50–64.

Richtsmeier JT, Cheverud JM, Dahaney SE, Corner BD, Lele S (1993*a*) The ontogeny of sexual dimorphism in the crab-eating macaque (*Macaca fascicularis*). *Journal of Human Evolution* **25**, 1–30.

Richtsmeier JT, Corner BD, Grausz HM, Cheverud JM, Dahaney SE (1993*b*) The role of post natal growth in the production of facial morphology. *Systematic Biology* **42**, 307–330.

Rohlf F, Bookstein FL (1990) *Proceedings of the Michigan Morphometrics Workshop*. Ann Arbor: University of Michigan Museum of Zoology.

Rohlf F, Slice DE (1990) Extensions of the Procrustes method for the optimal superimposition of landmarks. *Systematic Zoology* **39**, 40–59.

Shea BT (1983) Allometry and heterochrony in the African apes. *American Journal of Physical Anthropology* **62**, 275–289.

Shea BT (1986) Ontogenetic approaches to sexual dimorphism in the anthropoids. *Human Evolution* **1**, 97–110.

Schultz AH (1962) Metric changes and sex differences in primate skulls. *Yearbook of Physical Anthropology* **10**, 129–154.

Thompson D'AW (1917) *On Growth and Form*. Cambridge: Cambridge University Press.

Sneath PHA (1967) Trend surface analysis of transformation grids. *Journal of Zoology* (*London*) **151**, 65–122.

Sneath PHA, Sokal RR (1973) *Numerical Taxonomy*. San Francisco: W.H. Freeman.

Wood BA (1975) *An analysis of sexual dimorphism in primates*. Ph.D. Thesis, University of London.

Wood BA (1976) The nature and basis of sexual dimorphism in the primate skeleton. *Journal of Zoology*, *London* **180**, 15–34.

Wood BA (1985) Sexual dimorphism in the hominid fossil record. In *Human Sexual Dimorphism* (ed. Ghesquiere J, Martin RD, Newcombe F). London: Taylor and Francis.

Wood BA, Li Y, Willoughby C (1991) Intraspecific variation and sexual dimorphism in cranial and dental variables among higher primates and their bearing on the hominid fossil record. *Journal of Anatomy* **174**, 185–205.